FEBRUARY 1981 PPPL-1768
UC-20f

RADIATION LOSSES IN PLT DURING NEUTRAL BEAM AND ICRF HEATING EXPERIMENTS

PLASMA PHYSICS LABORATORY

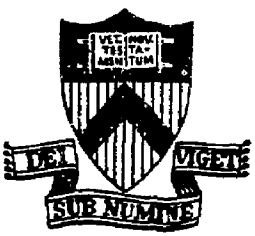

PRINCETON UNIVERSITY
PRINCETON, NEW JERSEY

This work supported by the U.S. Department of Energy Contract No. DE-AC02-76-CHO-3073. Reproduction, translation, publication, use and disposal, in whole or in part, by or for the United States Government is permitted.

Radiation Losses in PLT During Neutral Beam and ICRF Heating Experiments

S. Suckewer, E. Hinnov, D. Hwang, J. Schivell, G. L. Schmidt, K. Bol, N. Bretz, P. Colestock, D. Dimock, H. Eubank, R. Goldston, R. J. Hawryluk, J. Hosea, H. Hsuan, D. Johnson, E. Meservey, and D. McNeill

Plasma Physics Laboratory, Princeton University

Princeton, New Jersey USA 08544

ABSTRACT

Radiation and charge exchange losses in the PLT tokamak are compared for discharges with ohmic heating only (OH), and with additional heating by neutral beams (NB) or RF in the ion cyclotron frequency range (ICRF). Spectroscopic, bolometric and soft x-ray diagnostics were used. The effects of discharge cleaning, vacuum wall gettering, and rate of gas inlet on radiation losses from OH plasmas and the correlation between radiation from plasma core and edge temperatures are discussed.

For discharges with neutral beam injection the radiation dependence on type of injection (e.g., co-injection versus counter- and co- plus counter-injection) was investigated. Radial profiles of radiation loss were compared with profiles of power deposition. Although total radiation was in the range of 30-60% of total input power into relatively clean plasma, nevertheless only 10-20% of the total central input power to ions and electrons was radiated from the plasma core. The radiated power was increased mainly by increased influx of impurities, however a fraction of this radiation was due to the change in charge-state distribution associated with charge-exchange recombination.

During ICRF heating radiation losses were higher or comparable to those experienced during co- plus counter-injection at similar power levels. At

these low power levels of ICRF heating the total radiated power was ~ 80% of the auxiliary heating power. Radiation losses changed somewhat less rapidly than linearly with ICRF power input up to the maximum available at the time of these measurements (0.65 MW).

I. Introduction

The Princeton Large Torus (PLT) tokamak has been extensively operated with neutral beam [1] and with ion cyclotron resonance frequency (ICRF) [2] heating at power levels exceeding the ohmic power input (400-800 kW). Many operating conditions affect the plasma characteristics to a greater or lesser extent. For example, there are the various combinations of the four (tangential) neutral beams, about 500-800 kW each, of which two inject parallel to the ohmic heating current (co-injectors) and the other two antiparallel (counter-injectors). The ICRF power may be preferentially coupled to a minority ion in the plasma, e.g., H^+ or $^3He^{++}$ in deuterium plasma. There are variations of current, toroidal field, density and temperature, and impurity content of the ohmically-heated target plasma. The latter conditions are not independently variable. In particular, the impurity content depends on the limiter material (tungsten, stainless steel or graphite), on the previous history of the vacuum vessel (amount and manner of discharge cleaning, and gettering by evaporating titanium on the walls), and the programming of current and of gas inlet rate. The latter in turn affects the plasma density and temperature, and is implicitly restricted by plasma composition; e.g., high density, implying high gas inflow rate, is only possible if the carbon and oxygen concentrations are low.

Both the magnitude and the spatial distributions of radiated power is of course primarily determined by the impurity content. Light elements, oxygen and carbon, radiate strongly only near the periphery, as they become completely stripped in the hot interior of the plasma. On the other hand, radiation intensity from heavier elements is more uniform in radius or somewhat peaked toward the center, because the radiation efficiency is not

very strongly temperature dependent (in the temperature range of interest) and varies linearly with electron density.

In this paper we survey measured radiation intensities both in absolute magnitude and spatial distribution under a variety of target plasma and auxiliary heating conditions, and compare the measurements with corresponding power inputs deduced from measured total powers and calculated radial distributions. In view of the large variety of experimental conditions the data presented here are representative rather than comprehensive in nature.

II. Experimental Arrangement

A schematic view of the PLT tokamak and the principal diagnostic equipment is shown in Fig. 1. The quasi-steady part of the ohmically heated target plasma lasts about 0.7 sec, and usually toward the latter part of this interval the auxiliary power (NB or ICRF or both) is turned on for about 150 msec, which is sufficient to produce a new quasi-steady condition. The limiter is either graphite or stainless steel (in pre-1978 experiments tungsten). The vacuum vessel is stainless steel, with titanium evaporated on it at several toroidal locations, for the purpose of trapping oxygen and carbon, and providing greater flexibilty of gas inlet programming.

The energy emitted by the plasma in the radial direction, i.e., radiation and neutral atoms, is measured by means of bolometers: a stationary array viewing different chords simultaneously and a separate single bolometer, which can scan the chords from shot to shot [3]. The absolute magnitude of the measurement is subject to a calibration uncertainty of + 50%. Charge-exchange neutral atom flux is measured separately by charge-stripping energy analysers at high energies and time-of-flight measurements at low energies. Spectrum

line intensities are measured by a variety of spectrometers covering the entire range from soft x-rays to visible. All these spectrometers are calibrated for absolute intensity measurements.

Comparing the various measurements in time and space, it appears that resonance-line emission of various impurity ions constitutes the bulk of the bolometer signal, i.e., continuum emission and charge-exchanged neutrals provide only minor contributions. An exception to this may occur during high-power neutral beam injection, when charge-exchanged neutrals may be appreciable, because the bolometer is toroidally located (Fig. 1) between two injectors, where during injection the neutral hydrogen density is larger than toroidal average. However, no measurements distinguishing charge-exchange and radiation contributions in the bolometry signal have been feasible so far.

One further uncertainty in interpreting the radiation measurements is the assumption of toroidal and poloidal symmetry. Toroidally, there are two known singular locations: the limiter and the gas inlet valve. Because of the difficulty of access, their effect is only approximately known, but is probably largely peripheral, as would be expected from the high toroidal mobility of the ions. There are also known (measured) poloidal asymmetries [4,5], which may be quite large near the periphery but diminish rapidly toward the interior of the plasma. Such asymmetries do not strongly affect the measured total power but can alter the radial distribution of the local emissivity deduced by an Abel inversion. For the broad radiation profiles usually observed on PLT, simple numerical estimates indicate that the deduced central radiation levels represent essentially an upper limit.

Spectroscopic measurements do not suffer appreciably from this problem, because the various ions radiate strongly only over a limited electron temperature range, and hence only over a limited radial extent for discharges

with peaked temperature distributions. However, spectroscopic measurements comprise only a few of the strong resonance lines, and the rest of the radiation is estimated on the basis of various model calculations [6,7]. This procedure is generally quite reliable (unless some unknown element is present in significant quantities), but it is very laborious and therefore not practicable in surveys over a large variety of plasma conditions. It is therefore used mostly as a spot-check on the bolometry, in total radiation measurements.

The soft x-ray measurements [8] are somewhat intermediate between the bolometric and spectroscopic methods. The instrument measures the total photon flux at wavelengths shorter than about 300 Å, but at the longer-wavelength end of its sensitivity (where indeed a large fraction of the radiation is emitted) the photoefficiency is uncertain. It therefore measures fairly adequately the total radiation from the hot central part of the plasma, but tends to ignore the radiation from lower ionization potential ions further out. However, since the gross spectral characteristics of tokamak plasmas do not vary very strongly either with temperature or with composition, this instrument is very useful for monitoring relative changes as plasma conditions are varied.

In the present paper all these measurement methods are implicitly used, with primary emphasis in regards to bolometric measurements on the total energy flux. In these, poloidal variations are symmetrized, and toroidal variations ignored. The latter is expected to lead to an underestimate of the total radiated power, but probably not a very serious one.

III. Radiation in Ohmically Heated Plasma

In this section we review briefly the radiation characteristics in ohmically heated plasmas, which are in qualitative agreement with the results reported earlier [9] and by several other experiments [10-14].

In a plasma with high level of oxygen or carbon, the total radiation is high, but it is strongly concentrated near the periphery of the plasma. As a corollary, the edge temperature, the heavier element concentration, and central radiation are low, the central temperature is high, and the current channel and power input radial distribution are fairly narrow. Such discharges have generally good confinement, but they are unstable against raising the density by gas inflow.

Oxygen and carbon levels in the discharge may be reduced by discharge-cleaning techniques [15,16] and titanium gettering [17]. Reduction in oxygen and carbon results in raising the peripheral temperature and a concomitant increase in the wall and limiter materials in the discharge. With the limiter made of high-Z material, the central radiation is considerably higher, in some cases rising to a substantial fraction of the local power input. Such discharges, even when the total radiation is not very high, tend to have poor confinement, but they are generally more stable against gas influx and auxiliary heating, than the narrower oxygen-rich discharges. Intensive (hydrogen) gas inflow tends to lower the peripheral temperature and reduce the wall and limiter-material influx, while raising the plasma density. The rise in plasma density usually implies a lowering of temperature not only on the periphery but everywhere, partly because the power input tends to drop as a result of decreased effective ion charge.

To recapitulate, there appear to be three basic types of discharge 1) a narrow (peaked) low-density high-temperature discharge with the periphery cooled primarily by oxygen or carbon radiation, 2) a narrow high-density low-temperature discharge with periphery cooled by hydrogen influx and recycling, and 3) a wider, low-density moderate-to-low temperature discharge with considerable central radiation from heavier impurities. The third type may be converted to the first during a given discharge by adding a small puff of oxygen or neon [18], or to the second by adding a rather large puff of hydrogen [19]. These three types of discharge do not necessarily differ very much in total radiation, but they do differ in radial distribution and spectral origin.

IV. Radiation During Neutral Beam Injection

Many features of the radiation behavior observed in ohmic heating discharges also occur at least qualitatively with auxiliary heating. Figure 2 shows the correlation between peripheral temperature and the intensity of tungsten radiation (at a time when the limiter was still tungsten and tungsten radiation was a major mechanism of energy loss from the plasma interior). The radiation from the plasma interior falls mainly in the 30-70 Å region in the form of "tungsten bands" [20,21]; the temperature is of the ions measured from Doppler broadening of CIII lines within 2-3 cm from the limiter radius. The electron temperature behaves quite similarly. The data in Fig. 2 imply that the counter-beam tends to broaden the temperature (hence also ohmic heating current) radial profile, and the co-beam counteracts this effect; also that the principal tungsten release mechanism is not impact of the beam-ions directly on the limiter, but indirectly through modification of the plasma

properties, and also that the release of tungsten (or any limiter material) depends sensitively on the plasma edge temperature (presumably through formation of electron potential sheaths at the limiter). Because of the large radiation efficiency of tungsten ions, the tungsten limiters were replaced by interchangeable (in radial location) stainless steel and graphite limiters. Iron and chromium ions have a radiation pattern similar to tungsten, i.e. highest at highest electron density up to at least 2 keV temperature, but the radiation efficiency (per ion) is considerably lower. Carbon of course radiates strongly only near the periphery.

Figure 3 shows a representative sample of the radiation of the Fe XXIII ion (ionization potential, I.P., about 2 keV) before, during, and after neutral beam injection with steel and with carbon limiters respectively at comparable plasma density. The beam power was doubled in the case of the carbon limiter, and in general iron radiation is roughly proportional to beam power. Thus, there is about 3-4 times more iron in the discharge with steel limiters, but the relative changes and radial distributions are fairly similar. Experiments of this kind imply that the limiter is the principal, but not the sole source of metallic impurities in the plasma.

A representative case with steel limiter showing the differences between co- and counter injection at comparable power levels is described in Fig. 4 and 5. In this experiment, approximately 400 kW was injected between 400 and 500 msec into a plasma with ohmic heating power also about 400 kW (toroidal field 32 kG, current about 400 kA, line-average density 2.6×10^{13} cm^{-3}, steel limiters at r = 40 cm). Figure 4 shows the radial profiles of electron temperature and density deduced from Thomson scattering measurements [22] at the end of the beam-injection, compared to the profiles at the same time without the beams. The data are averaged over several discharges, and

symmetrized over top and bottom halves with considerable variations in both respects. The results are probably quite reliable at $r < 25$ cm, but at larger radii they may be taken only as a rough indication of the trends. The electron densities apparently were not appreciably changed by the beams, except for a possible increase near the periphery. With the co-beam the electron temperature also did not change except for a modest increase at intermediate radii. With the counter-beam, however, the profile is significantly different, with substantially lower temperatures near the center and indications of higher temperatures and flatter slope near the periphery. Although the peripheral measurements are very uncertain, the indicated values are entirely consistent with the ion temperature measurements made under similar conditions with both steel and graphite limiters and also with the data shown in Fig. 2 for the tungsten limiter case. The change of the temperature profile of course implies a corresponding change in the current density, ohmic power input, and poloidal field distributions. The poloidal field distribution in turn presumably affects the radial transport rate and hence influences further the temperature distribution as well as the particle flux to the limiter.

The changes of brightness distribution of two iron ion resonance lines is shown in Fig. 5. The distribution without the beam injection was not measured, but it was probably very similar to the "before NB" curves, except perhaps slightly wider for the FeXXIII line. The scan is mechanically limited to $r < 17$ cm, so the outer edge of the FeXV could not be reached. We therefore show only the chord brightness for both ions, i.e., the number of photons emitted per cm^2 column along the line of sight. Since the radial position of each type of ion is limited to a range over which the electron density does not change very much and since the excitation rate is nearly

independent of electron temperature for the lines under consideration, the chord brightness is also proportional to the number of the corresponding ions along the line of sight.

The results clearly indicate a substantial difference in the iron concentrations between the co- and counter-injection cases, being roughly double in the latter case. The changes are quite similar in the near-central FeXXIII and the FeXV ions, the latter peaking in intensity in the neighborhood of $r \sim 25$ cm, i.e., the change (as well as the initial concentrations, which may be estimated from the absolute brightness values) appears to be homogeneous. [A slight relative increase of the FeXXIII concentration would be expected from the $T_e(r)$ change in the counter-injection case because somewhat less of the total iron ions would be in the higher, FeXXIV, XXV states].

The soft x-ray signals from these discharges were very similar to the FeXXIII light (in time-behavior as well as magnitude changes), indicating a small increase with the co-beam and roughly doubling with the counter-beam. The bolometry measurements [3,22] indicated a substantial central radiation peak in the counter-injection, and a fairly flat distribution or perhaps a small central peak in the co-injection case. Measurements of this type have been interpreted to indicate relative accummulation of heavy impurities in the center of the discharge with counter beam injection [24, 25]. Such interpretations do not seem to be warranted, and are certainly not compelling. We note that the radiation pattern of a heavier impurity such as iron, with a homogeneous concentration, behaves roughly as $n_e^2(r)$, whereas emission from oxygen, carbon (and hydrogen, including charge-exchanged neutrals) have a centrally hollow radiation profile. Thus a factor of 2-3 increase in the heavy impurity concentration may well produce an impressive central radiation peak without relative accumulation.

The increase of central radiation in high power neutral beam (co- or counter-) heating plasma may be further aggravated by the charge-exchange recombination [26] with beam injected neutral atoms, which tends to suppress the ionization balance to lower, more strongly radiating states.

The cause and effect relationship between increased (central) radiation levels and modification of the radial temperature profile in counter-injection (vs. co-injection) cases is not clearly established. However, in low-density discharges with steel limiters the radiation constiutes a substantial fraction of the power input into the electrons, thereby tending to lower the central conductivity and ohmic power input, thus further flattening the temperature profile and presumably causing higher influx of the limiter material by raising the edge temperature.

As illustrated in Fig. 6 differences in total radiated power between co- and counter-injection persist over a wide range of injected beam power, even when carbon limiters are used. The solid dots are based on spectroscopic line intensity measurements, the triangles on bolometric measurements, and the open circles on soft x-ray measurements. The latter, because they do not include the longer-wavelength radiation (e.g., oxygen resonance lines) near the periphery, have been normalized to bolometric measurements at beam power of 0.5 MW. The rather remarkable agreement between the different measurements indicates that line radiation is the dominant part of the total, and that the spectral character (i.e. relationship of longer-wavelength to shorter-wavelength radiation) of the emission does not vary appreciably with the power level.

The larger radiation with counter injection is undoubtedly due to higher impurity concentration in the plasma, and this in turn appears to be caused by higher edge temperature, or more generally a different radial temperature and power input distribution.

Generally, bolometer measurements on PLT account for between 30 and 60% of the total input power (P_b plus P_{OH}). Calculated thermal charge-exchange losses normally equal 25 to 50% of these measurements. Beam charge-exchange and orbit losses are not viewed by the bolometer. Radiation losses after a correction for charge-exchange account for between 30 and 50% of the input power to the electrons. If no correction is made for charge-exchange, from 40 to 80% of the electron input power is accounted for.

In order to minimize central radiation, practically all the experiments with auxiliary heating have been performed with graphite limiters and vacuum vessel wall conditioned by low-current discharge cleaning and titanium gettering (see [1], [27], [28]). Under these conditions, the central radiated power is generally a small fraction (10-20%) of the local power input. In some cases, however, it can still be a significant fraction of the total power input. Figure 7 shows some typical examples of radiated power deduced from bolometric measurements, and power input calculated from discharge parameters: the ohmic heating power density from a magnetic diffusion equation [29] using experimental electron temperature profile, loop voltage and toroidal current, and the beam power deposition from a Monte-Carlo simulation [30] of the beam absorption and thermalization.

In Figure 7, the injection was by 2 co- and 2 counter-beams, for a total beam-power of 2.1 MW. The ohmic heating power, initially about 0.5 MW decreased to about 0.3 MW because of increased electron temperature (and conductivity). The increase in radiation during the beam injection is to a large extent due to increased plasma density, rather than any dramatic change in impurity concentrations (central electron density increases from 2.3 to 4.5 x 10^{13} cm^{-3} during neutral beam injection). Thus, during the injection as before, the power is largely deposited in the plasma interior where radiation

losses are small but not entirely negligible, the outward energy flows by thermal conduction and particle transport, near the periphery the energy transport is augmented by a substantial amount of radiation, which helps to depress the edge temperature. In the insert the total input and radiated power before and during injection is shown.

Data in Fig. 6 represents a relatively high level of total radiation, especially during counter-beam injection. However, in PLT, a wide range of total radiation losses have been observed. In Fig. 8 are shown measurements for relatively low level of total radiation. Long term titanium gettering, vacuum vessel wall conditioning, and the use of carbon limiters all contributed to the reduction in total radiation losses. It is remarkable that even at a neutral beam power level of 2.8 MW the increase in radiation loss, ΔP_{rad}, did not exceed 0.7 MW. Central radiation losses in this case were also low and were found to decrease with increasing electron density [28]. This dependence is illustrated in Fig. 9 and results from a lower influx of high-Z impurities with increasing density. In this case, total radiation losses were rather independent of density. Such low radiation losses make possible a substantial increase in central electron temperature, from 1.2 to 2.5 keV for $P_b \approx 2.8$ MW at $\bar{n}_e \approx 3 \times 10^{13}$ cm^{-3}.

V. Radiation Losses During ICRF Heating

The ICRF heating in PLT [31] is in some modes similar to neutral beam heating. For example, rf power can be preferentially coupled to a minority ion in the plasma, e.g., H^+ or $^3He^{++}$ in deuterium, and creates a high-energy ions which then heat the bulk of the plasma by collisional thermalization, as in neutral beam injection. The ICRF heating has several potential advantages

over neutral beams, such as greater flexibility in choosing the location of applied power input, less bulky equipment near the tokamak, and the absence of significant introduction of neutral atoms in the hot center of the plasma, but to date the available power has been much less, and the available 25 MHz frequency is not optimal for PLT experiments.

Figure 10 shows the radiated power and power input in a D^+ plasma with 5% H^+ minority at 360 kW rf power. The radiated power is measured bolometrically, the power input is calculated from a ray-tracing code and a Fokker-Planck model for the minority-ion heating [32]. The qualitative similarity to neutral beam results, Fig. 7, is evident. In particular, the central radiated power remains quite small compared to power input, although the total (mostly peripheral radiation, especially during the rf heating) is significant and undoubtedly contributes to the lowering of the edge temperature (the vacuum vessel wall was conditioned in the same way as for NB injection). Analogous data for a rather low-power heating of $^3He^{++}$ minority ions, together with radial ion temperature profiles, are shown in Fig. 11. This experiment was characterized by an unusually large, almost 5 eV/kW, ion heating efficiency (roughly double the usual H^+ minority heating results). The electron temperature did not change very much in this experiment (as would be expected from the low power input), but the electron density roughly doubled which contribute some increase in T_i. Thus the increase of radiated power is to a large extent ascribable to the density increase, rather than change in plasma composition. The ion temperature radial profile was determined from the Doppler profiles of the indicated ion lines, measured with a rapid-scan spectrometer, which provides the time-evolution of a given line profile in a single discharge. The radial locations of the ions, determined by their ionization potentials and the electron temperature radial profile

were obtained from line emissivity radial distribution measurement. From the carbon line measurements it is evident that the absolute change in the perpiheral temperature was small. The near-central temperatures deduced from neutron emission and from the charge-exchanged D° energy distribution are in good agreement with the Doppler ion temperature, (the actual agreement is probably better than the figure shows, because the charge-exchange temperature measurement was performed at a different time, when the plasma conditions had changed in a direction where lower T_i would be expected).

The variation of total radiation with ICRF power is shown in Fig. 12. As in the neutral-beam data (Fig. 6) the soft x-ray measurements have been normalized to bolometry at one point. In these measurements the central electron density increased from 2-3 x 10^{13} cm^{-3} before to 4-5 x 10^{13} cm^{-3} during the ICRF heating, and the central electron temperature increased slightly, from about 1.4 keV to 1.5 keV. Total accountable radiation losses were not greater than 50% of total input power for any rf power presented in Fig. 12. Detailed comparisons of changes of temperature profile, and particularly the edge temperature would be desirable, especially when higher power input levels become available.

VI. Conclusions

Although there are many variations of detail depending on particular conditions and previous history, the principal features of the power radiated with auxiliary heating appear to be as follows:

1. The total radiated power increases with power input slightly less rapidly than linearly.

2. The power input occurs mostly in the interior of the plasma, whereas the radiated power arises to a large extent near the periphery. With a few exceptions noted below the radiated energy from the interior, i.e., energy that is lost immediately, constitutes a small fraction (less than 20%), of the total local power input. Thus the bulk of the input energy resides in the plasma for about one confinement time, causing a rise in the interior temperature (even if the total radiated power is equal to the total power input), and it is transported from the interior to the periphery as particle kinetic energy.
3. The principal exception to this description occurred in the low-density discharges with tungsten limiters, where radiation losses were overwhelmingly important everywhere, sometimes even causing the hollow electron temperature profiles. An additional exception is the low-density discharge with steel limiters, where radiated power may be a considerable fraction of the power input into electrons.
4. The central radiated power (and to a lesser extent the total radiated power) is inversely correlated with the electron density and peripheral plasma temperature. High-density plasmas tend to have low central radiation levels because the rapid (hydrogen) gas inflow and recycling, required to produce and maintain high-density discharges, also depress the peripheral temperatures, and hence impurity content.
5. In neutral beam heating counter-injection produces significantly higher radiation losses than either co-injection or simultaneous co- and counter-injection at the same power level, probably because counter-injection tends to produce higher peripheral temperature (flatter radial profile).

6. ICRF heating produces radiation losses higher or comparable to co-plus counter-injected neutral beam at the same (< 1 MW) power level. Although the radiation is higher than in the neutral beam case, heating efficiency has not been substantially affected, since the radiation in the plasma interior remains generally a small fractions of the total power input.

Thus, in general terms radiation effects with auxiliary heating are similar to ohmic heating alone. The effect may be either unfavorable or favorable (by reducing peripheral temprature) for the purpose of producing high-temperature plasma. Usually, the radiation level is not very important in influencing the plasma dynamics, especially near the center of the plasma, but it is sufficiently high that a factor 2-3 increase of central radiation cannot be tolerated.

Acknowledgments

We wish to express our appreciation to S. Von Goeler and N. Sauthoff for making available their soft x-ray data, F. Jobes and J. Strachan for operating PLT, Neutral Bear and ICRF Teams for auxiliary heating, and M. Stodiek for general PLT guidance and keeping PLT alive. We would also like to express our thanks to J. McEnerney for his computational support.

REFERENCES

[1] EJBANK, H., et. al., Phys. Rev. Lett 43 (1979) 270.

[2] HOSEA, J., et al., Course and Workshop on Physics of Plasmas Close to Thermonculear Conditions, Varenna, Italy, 1979, Editrice Compositori, Bologna (1980).

[3] HSUAN, H., HWANG, D., SCHIVELL, J., and SCHMIDT, G., Bull. Am. Phys. Soc. 24 (1978) 1107.

[4] TERRY, J., MARMAR, E., CHEN, K., and MOOS, H., Phys. Rev. Lett 39 (1977) 1615.

[5] SUCKEWER, S., HINNOV, E., and SCHIVELL, J., Princeton University, Plasma Physics Laboratory Report, PPPL-1430 (1978).

[6] EQUIPE TFR, Nucl. Fusion 15 (1975) 1053.

[7] HINNOV, E., SUCKEWER, S., BOL, K., HAWRYLUK, R., HOSEA, J., and MESERVEY, E., Plasma Physics 20 (1978) 723.

[8] VON GOELER, S., SAUTHOFF, N., BITTER, M., et al., Princeton University, Plasma Physics Laboratory Report, PPPL-1308 (1977).

[9] HSUAN, H., et al., Proc. Joint Varenna and Grenoble Int. Symp. on Heating in Toroidal Plasmas, Grenoble (1978).

[10] MESERVEY, E., BRETZ, N., DIMOCK, D., and HINNOV, E., Nucl. Fusion 16 593 (1976).

[11] FIELDING, S., HUGILL, J., McCRACKEN, G., et al., Nucl. Fusion 17 (1977) 1382.

[12] TFR GROUP, J. Nucl. Mater. 74, #2 (1978).

[13] TFR GROUP, Nucl. Fusion 17 (1977) 1187.

[14] MURAKAMI, M., et al., Phys. Rev. Lett. 42 (1979) 655.

[15] OREN, L. and TAYLOR, R. J., Nucl. Fusion 17 (1977) 1143.

[16] DYLLA, F., et al., J. of Vac. Sci. and Technol. 17 (1980).

[17] STOTT, P., DAUGHNEY, C., and ELLIS, R., Nucl. Fusion 15 (1975) 431.

[18] BOL, K., et al., Nucl. Fusion 18 (1978).

[19] HINNOV, E., et al., Bull. Am. Phys. Soc. 24 (1979) 1173.

[20] ISLER, R. C., NEIDIGH, R.V., and COWAN, R.D., Phys. Lett. A63 (1977) 295.

[21] HINNOV, E., and MATTIOLI, M., Phys. Lett. A66 (1978) 109.

[22] GRISHMAH, L., HSUAN, H. and SCHMIDT, G., (submitted for publication).

[23] BRETZ, N., DIMOCK, D., FOOTE, S., JOHNSON, D, LONG, D., and TOLNAS, E., Applied Optics 17 (1978) 192.

[24] ISLER, R. C., CRUME, E. C., ARNURIUS, D.E., and MURRAY, L.E., Oak Ridge National Laboratory Report ORNL/TM-7472 (1980).

[25] EAMES, D., VON GOELER, S., et al., Bull. Am. Phys. Soc. 25 (1980) 998.

[26] SUCKEWER, S., HINNOV, E., BITTER, M., HULSE, R., and POST, D., Phys. Rev A22 (1980) 725.

[27] EUBANK, H., et al., Proc. of Joint Varenna-Grenoble Conference on Heating in Toroidal Plasmas, Como, Italy (1980).

[28] GOLDSTON, R., et al., ibid.

[29] HAWRYLUK, R. J., in "Course on Physics of Plasma Close to thermonuclear Condition", Varenna, Italy (1979) (to be published by Pergammon Press).

[30] GOLDSTON, R. J., McCUNE, D. C., TOWNER, H. H., DAVIS, S. L., HAWRYLUK, R. J., and SCHMIDT, G. L., (to be published).

[31] HOSEA, J. et al., Proc. of 8th Intern. Conf. on Plasma Physics and Controlled Fusion Research, Brussels, 1-10 July, 1980.

[32] COLESTOCK, P., Bull. Am. Phys. Soc. 24, 1073 (1979); also HWANG, D., et al., Proc. IV International Conference on Plasma Physics, Nagoya, Japan 1980.

FIGURE CAPTION

Fig. 1. Locations of the major diagnostics around PLT in relation to neutral beam injection and ICRF wave antenna.

Fig. 2. Intensity of tungsten radiation versus ion edge temperature for different neutral beam injection conditions (co-beam ~ 500 kW, Ctr-beam ~ 350 kW, P_{OH} ~ 600 kW).

Fig. 3. Sample of the radiation of the FeXXIII ion before, during, and after neutral beam injection with steel (co + ctr -injection) and carbon (2co + 2ctr-injection) limiters (note different ordinate scales).

Fig. 4. Radial profiles of electron temperature and density before and during neutral beam co- and counter injection (steel limiter).

Fig. 5. Brightness distribution of FeXXIII and FeXV resonance lines before and during neutral beam co- and counter-injections.

Fig. 6. Total radiation losses in the PLT versus neutral beam injected power during co-, ctr -, and co + ctr-injection [$\bar{n}_e$ = (1.5 - 2) x 10^{13} cm^{-3}].

Fig. 7. Radial profile of measured radiation losses and calculated input power before and during neutral beam injections for P_b = 2.1 MW (2co + 2 ctr).

Fig. 8. Total radiation losses in the PLT versus neutral beam injected power during co-, ctr-, and co + ctr-injection.

Fig. 9 Central plasma radiation versus electron density for 4 (2.7 MW) and 2 (1.4 MW) neutral beam injection, and for ohmic heating (OH) only discharges.

Fig. 10. Radial profile of measured radiation losses and calculated input power before and during ICRF heating experiment with hydrogen as minority heated.

Fig. 11. (a) Radial profile of radiation losses and input power during and before ICRF heating with ^{3}He as minority.

(b) Corresponding measured ion temperature profile.

Fig. 12. Total impurity radiation losses during ICRF heating experiments versus input power.

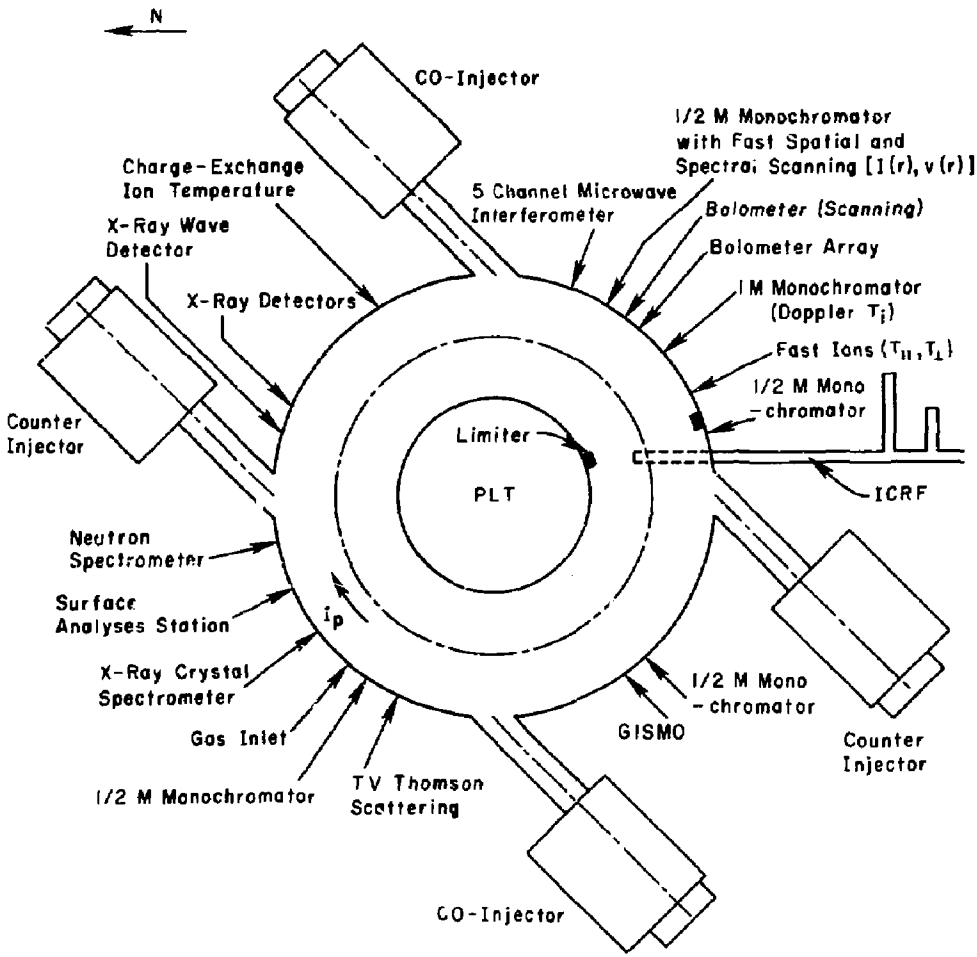

Fig. 1. (PPPL-806814)

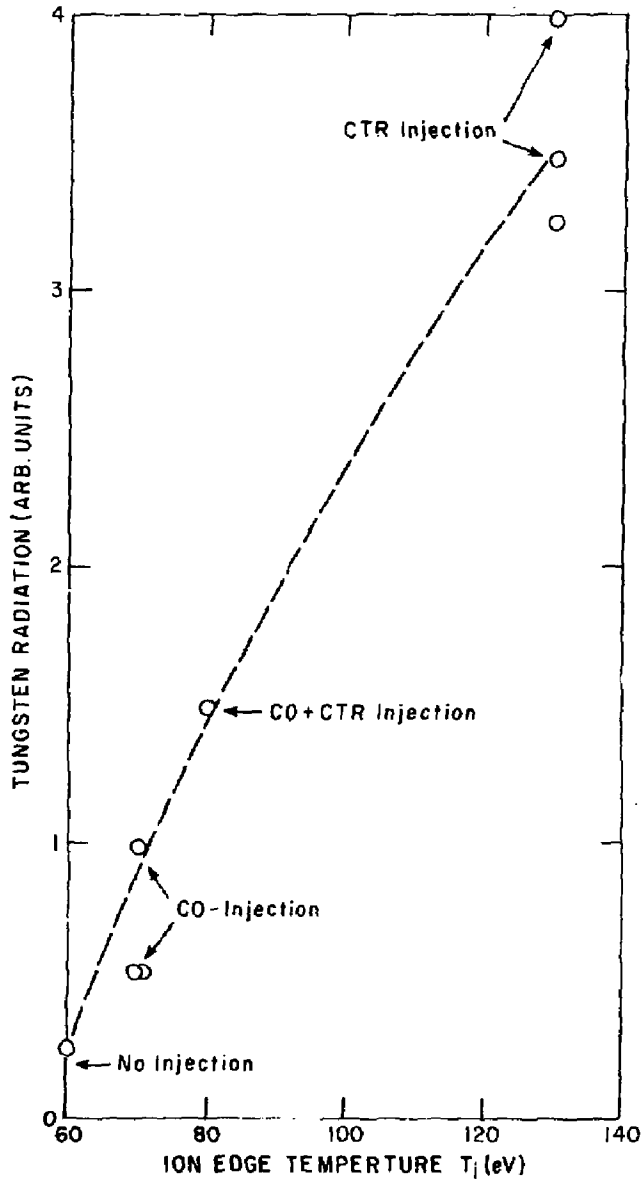

Fig. 2. (PPPL-783498)

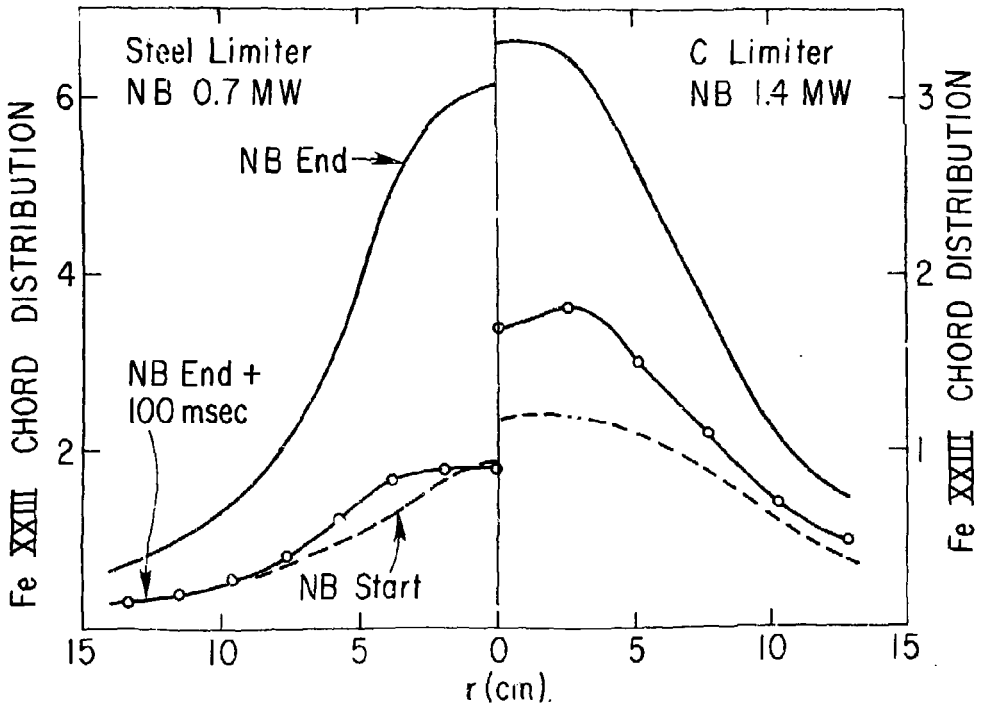

Fig. 3. (PPPL-786196)

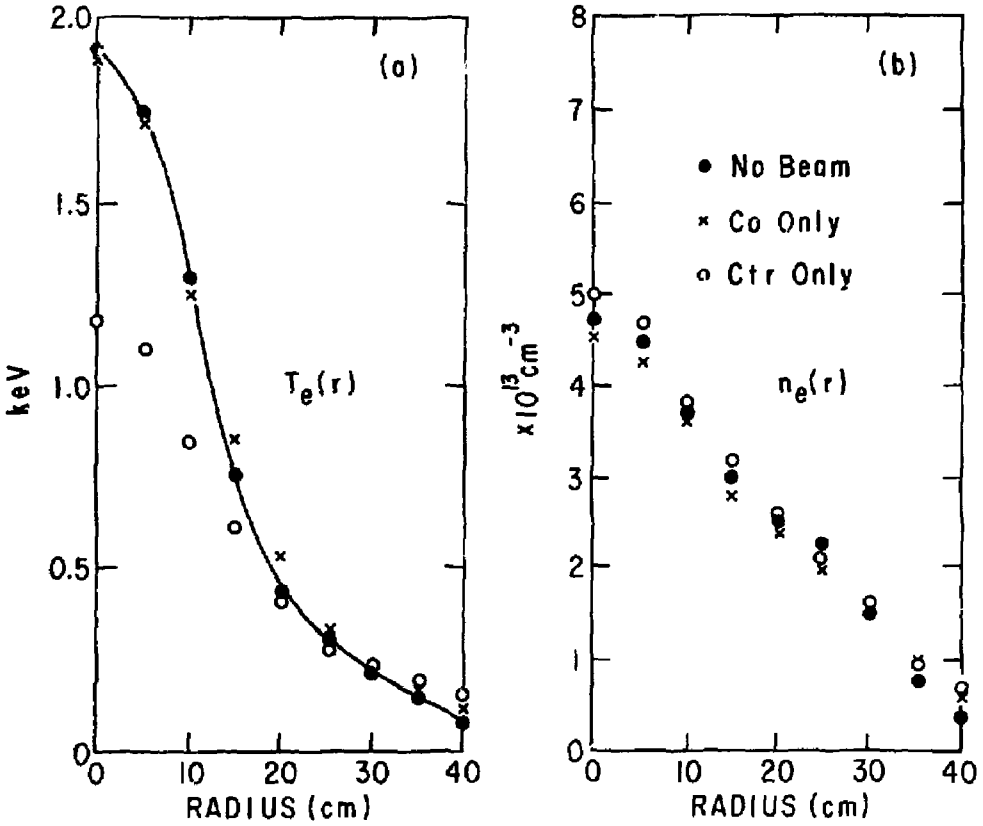

Fig. 4. (PPPL-806826)

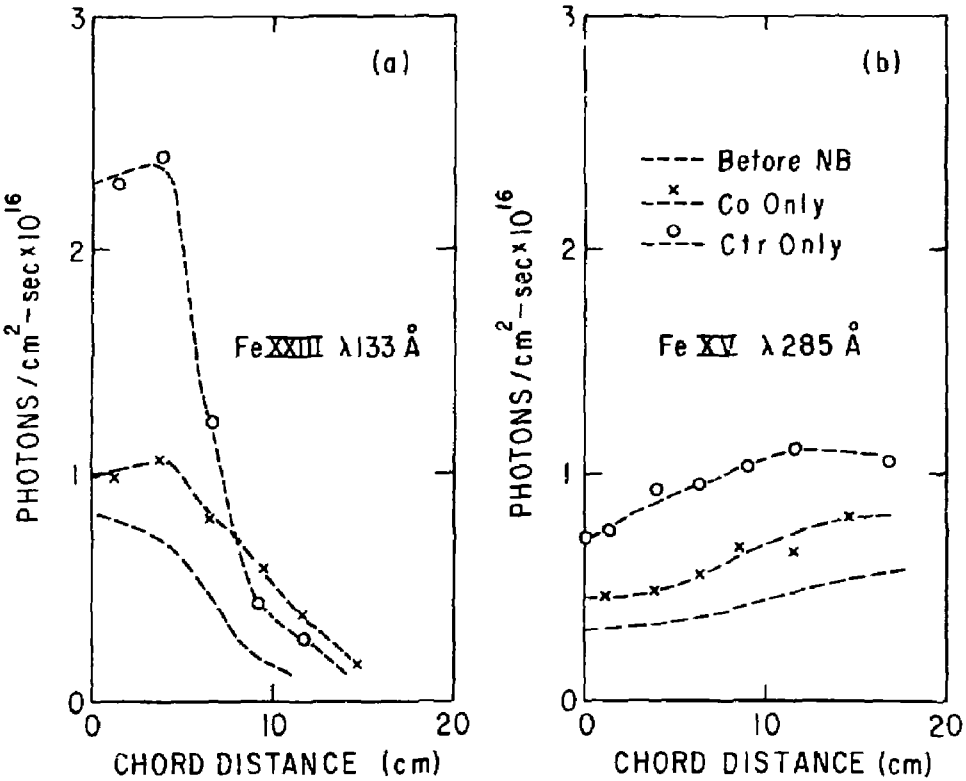

Fig. 5. (PPPL-806?25)

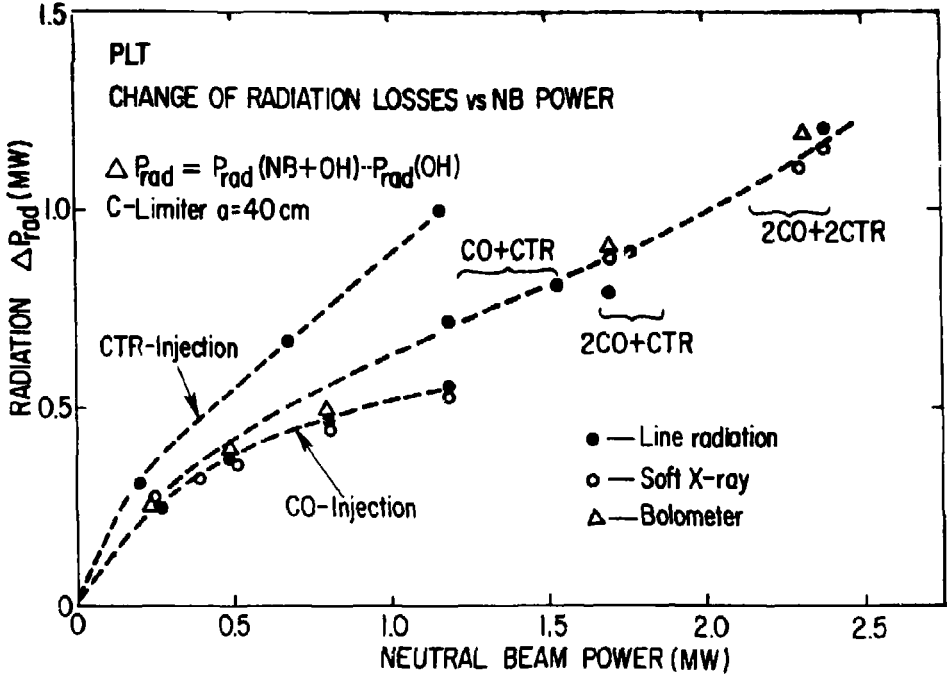

Fig. 6. (PPPL-806809)

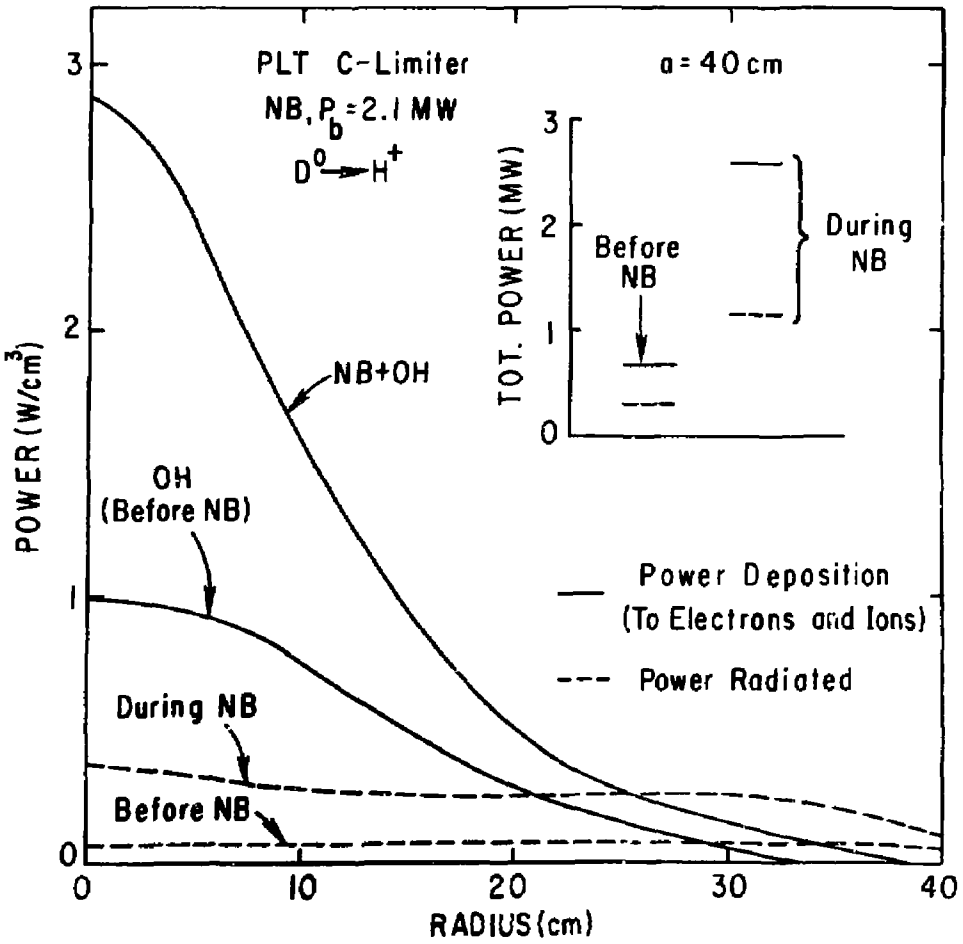

Fig. 7. (PPPL-796398)

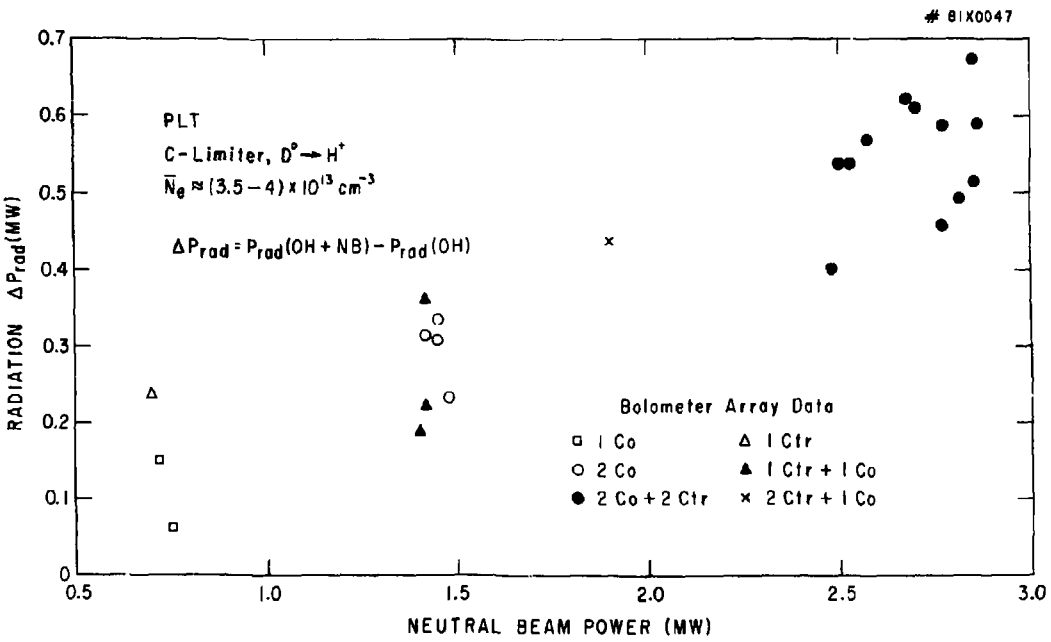
81X0047
PLT
C-Limiter, D° → H⁺
$\bar{N}_e \approx (3.5-4) \times 10^{13}\ cm^{-3}$
$\Delta P_{rad} = P_{rad}(OH+NB) - P_{rad}(OH)$
Bolometer Array Data
□ 1 Co
△ 1 Ctr
○ 2 Co
▲ 1 Ctr + 1 Co
● 2 Co + 2 Ctr
× 2 Ctr + 1 Co
RADIATION ΔP_{rad}(MW)
NEUTRAL BEAM POWER (MW)
0
0.1
0.2
0.3
0.4
0.5
0.6
0.7
0.5
1.0
1.5
2.0
2.5
3.0

Fig. 8.

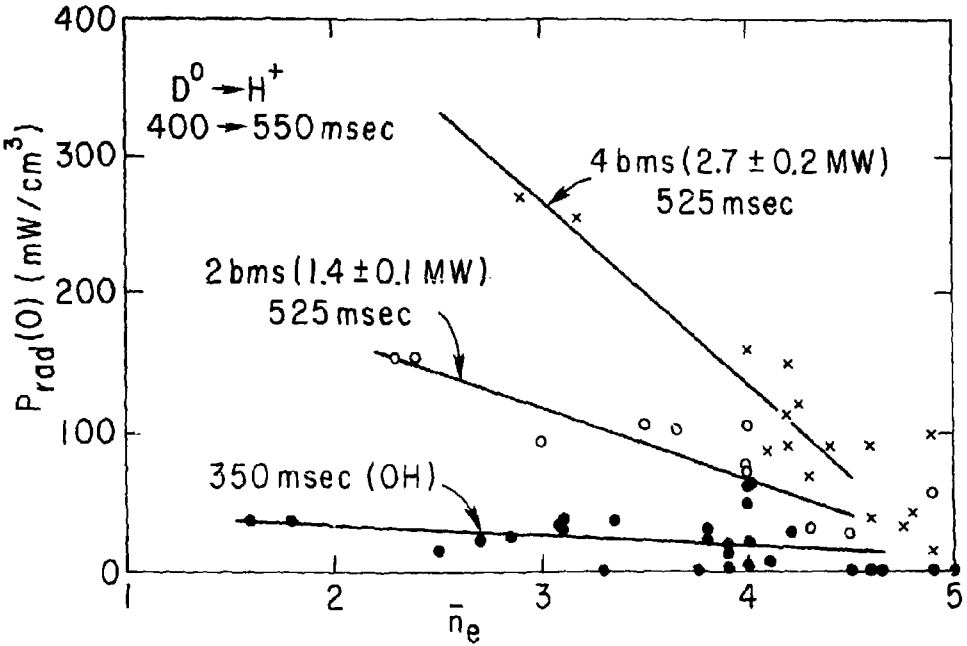

Fig. 9. (PPPL-806368)

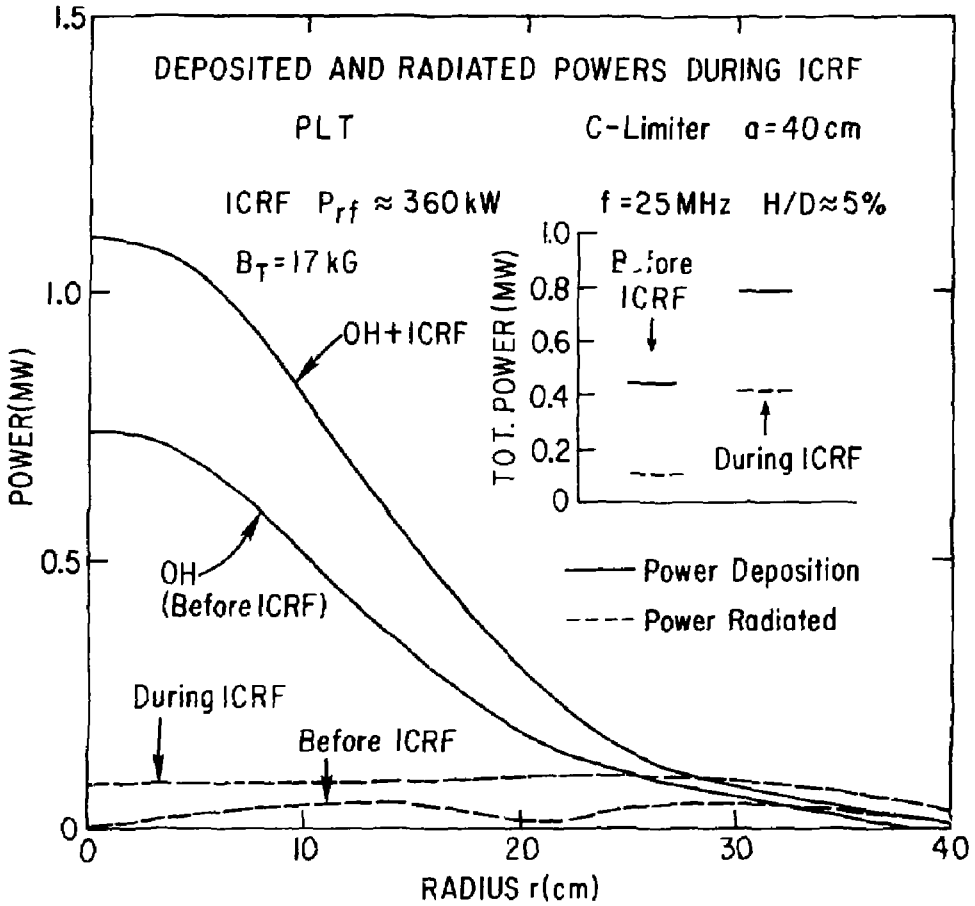

Fig. 10. (PPPL-809072)

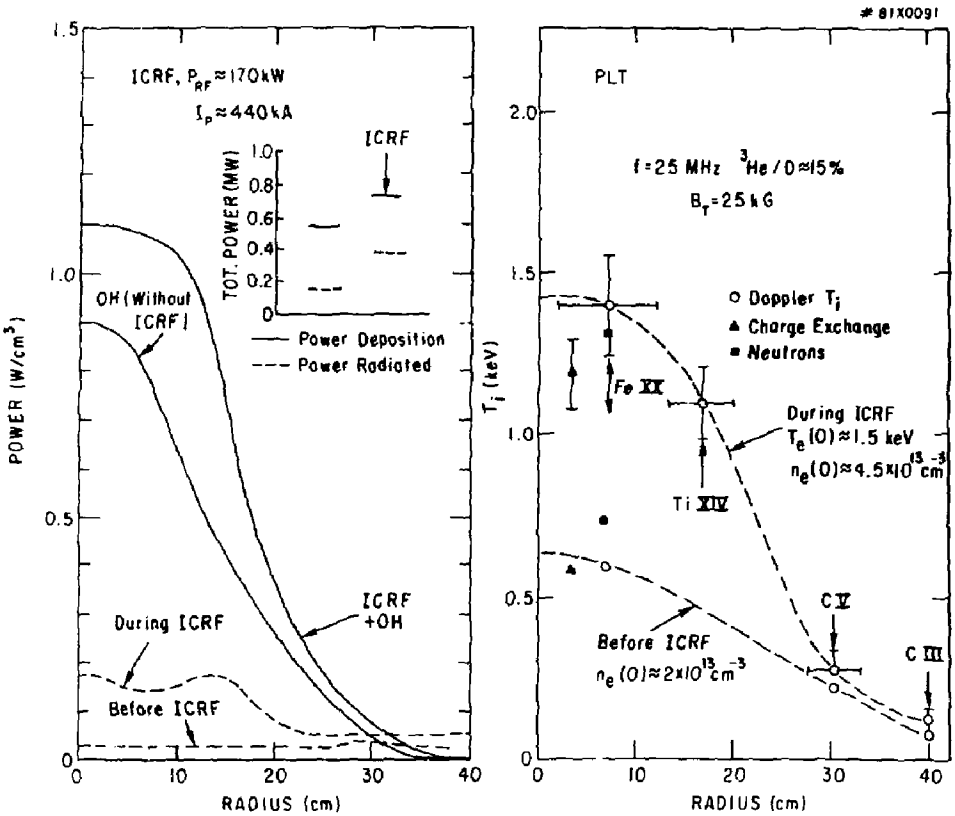
#81X0091
ICRF, P_{RF}≈170kW
I_p≈440kA
ICRF
TOT. POWER (MW)
Power Deposition
Power Radiated
OH (Without ICRF)
During ICRF
Before ICRF
ICRF +OH
POWER (W/cm³)
RADIUS (cm)
PLT
f=25 MHz ³He/D≈15%
B_T=2.5 kG
Doppler T_i
Charge Exchange
Neutrons
Fe XX
Ti XIV
During ICRF
$T_e(0)$≈1.5 keV
$n_e(0)$≈4.5×10¹³ cm⁻³
Before ICRF
$n_e(0)$≈2×10¹³ cm⁻³
C VI
C III
T_i (keV)
RADIUS (cm)

Fig. 11.

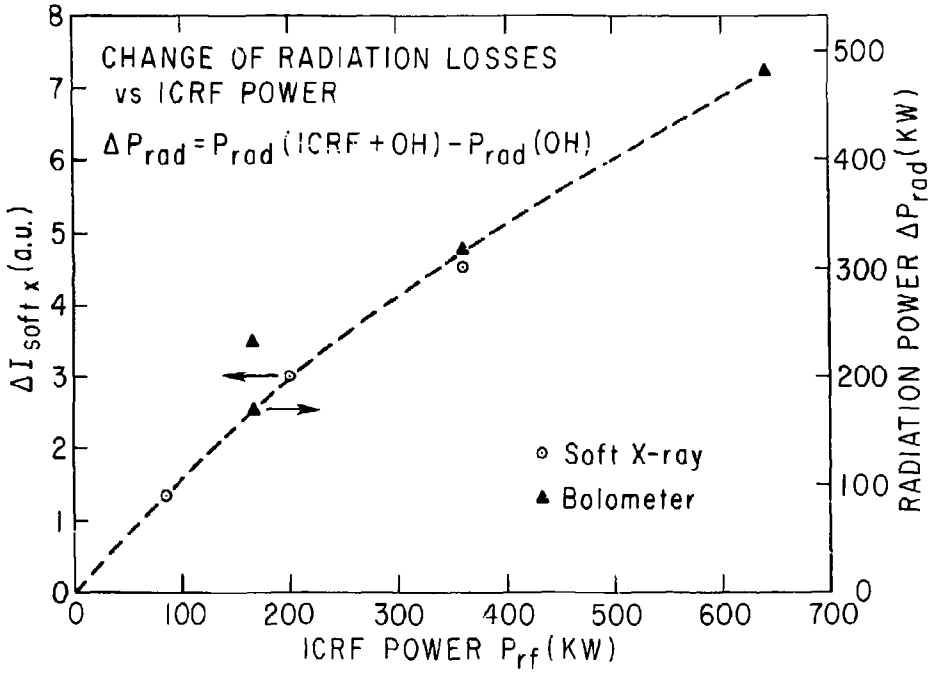

Fig. 12. (PPPL-803639)